

The Definition of Mini Labyrinth Benchmark for Radiation Shielding Calculations

Branislav Vrbán¹

¹Slovak University of Technology in Bratislava, Institute of Nuclear and Physical Engineering
Ilkovičova 3
81219, Bratislava, Slovakia
branislav.vrbán@stuba.sk

Štefan Čerba¹, **Jakub Lúley**¹, **Vendula Filová**¹, **Vladimír Nečas**¹, **Erwan Radenac**²

²École Nationale des Mines de saint Etienne
42023 Saint-Étienne Cedex 2
France

stefan.cerba@stuba.sk, jakub.luley@stuba.sk, vendula.filova@stuba.sk,
vladimir.necas@stuba.sk, erwan.radenac@laposte.net

ABSTRACT

The Mini Labyrinth experiment is a neutron and gamma shielding experiment constructed at the Slovak University of Technology, Bratislava (STU). The STU Mini Labyrinth consists of NEUTRONSTOP shielding blocks, blocks of moderators, various neutron sources, and a graphite prism. This paper gives the definition of the Mini Labyrinth V2 experiment which enables its modelling in the state-of-art transport codes and presents the newest experimental results of neutron and gamma field measurements and introduces the V3 version currently being developed. Various neutron and gamma detectors are used for the measurement including the Thermo Scientific RadEye portable survey meter, the SNM-11 boron-coated corona detector, the He3 tube detector, and CR-39 track detectors. As for the main results, the relative change of the mesh tallies of total neutron flux from MONACO CE and MCNP CE simulations in V2 geometry is acceptable and well below 2 %. The one sigma range of cross-section induced uncertainty to the ambient dose equivalent from neutrons was estimated to 1.48 % photons of 0.59 %). The measurement of neutron related quantities showed the relevant influence of the room effect, the almost perfect match was achieved in the case of comparison of normalized photon count rates.

1 INTRODUCTION

The use of ionizing radiation in various fields brings enormous benefits to people when it is used safely. However, the risk associated with radiation needs to be controlled and mitigated. To achieve the stated goals there has been significant development of methods and approaches used in the calculation of radiation shielding. At first, modelling of relevant effects for radiation protection was primarily focused on analytical modelling of particle transmission through relevant materials in simple geometries. However, with time the focus was shifted to simulation and the modelling of the complex geometries utilizing the so-called primary principles and their stochastic nature. The radiation shielding modelling is highly dependent on the computer codes and their capabilities. This leads to the necessity of knowing the accuracy of these computation codes and the proper use of nuclear data. Furthermore, it is highly desirable to evaluate the user effect on the final obtained shielding parameters. One of the most

effective ways of evaluating the validity of the used computational codes and nuclear data, is the designing and construction of relevant benchmark experiments. This paper offers a detailed description of the Mini Labyrinth benchmark being developed at Slovak University of Technology in Bratislava (STU). In addition, further benchmark upgrades are shortly introduced. The aim of this work is to contribute to the Shielding Integral Benchmark Archive and Database (SINBAD) which contains compilations for experiments related to reactor shielding, fusion neutronics shielding and accelerator shielding experiments. The work on SINBAD is jointly carried out by the United States' Radiation Safety Information Computational Center (RSICC) and the NEA. The main conclusions and drawbacks found during the quality review of the database can be found in [1].

2 THE MINI LABYRINTH V2

The STU Mini Labyrinth is inspired by the ALARM-CF-AIR-LAB-001 ICSBEP experiment [2] and is constructed to allow the validation of computational codes against the experimental measurements. In parallel, the relevant experience, understanding, and performance testing of the various radiation detectors can be gained. The experimental setup comprises the PuBe neutron source with the emission rate of $1.06E7 \text{ n.s}^{-1}$, several NEUTRONSTOP [3] 6x12x25 cm C-shape shielding blocks (polyethylene with 5 % boron), H₂O filled PLA tank, plastic source holder, graphite prism, and radiation detectors. The neutron source can be placed in two positions. The insertion in the first position is from the left, from the corridor of the labyrinth. The second position is on the right, into the adjustable cavity inside of the graphite prism. By filling the PLA tank with light water or by adjusting the thickness of the graphite block facing the labyrinth, the experimenter may significantly vary the neutron spectra in the labyrinth corridors and thus can make a principally new benchmark case. The details of the source holder and PLA tank can be found in Fig. 2.

2.1 Geometry model - V2

As the Mini labyrinth experiment is developed step-by-step, also several geometry versions have been defined. The very first version (V1) consisting of NEUTRONSTOP blocks, moderator tank and one neutron source position was designed to evaluate basic design principles [4]. The second version (denote as V2) was extended by a graphite prism to produce thermal neutrons. From the V2 version of the Mini Labyrinth also a benchmark geometry was defined, which is shown in Fig. 1.

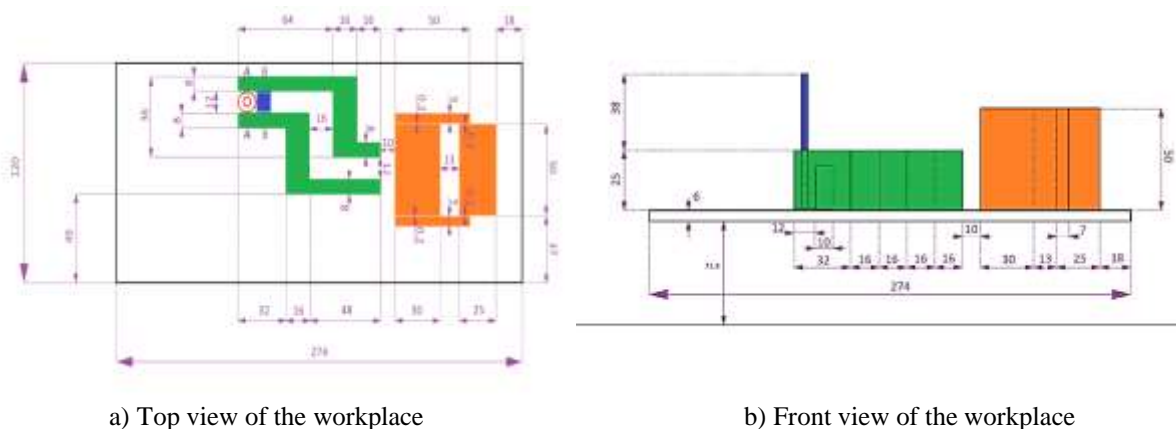


Figure 1: Geometry definition of the benchmark (dimensions are in cm) [5]

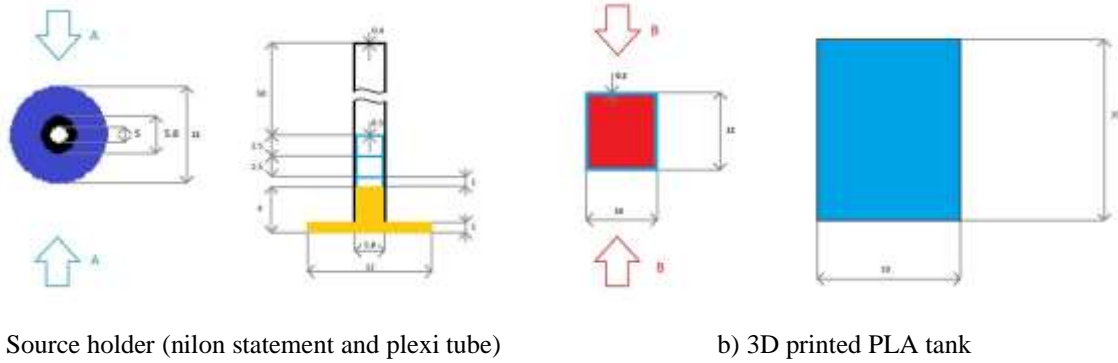


Figure 2: Details of the source holder and PLA tank [5]

Several different detectors are available for the measurement of the gamma and neutron fields. The Thermo Scientific RadEye SPRD-GN [6] dose meter is usually placed on a PLA holder, which can be seen in Fig. 3-a). Neutron detectors, such as the SNM-11 boron-coated corona detector or the SI-19N He3-tube can be hung on their cables from above of the Mini Labyrinth during measurement. In terms of dimensions, SNM-11 has 1.8 cm in diameter and 33.5 cm in length. The SI-19N He-3 neutron detector has 15.24 cm in length and 3.175 cm in diameter and is filled with helium at 4 atm pressure.

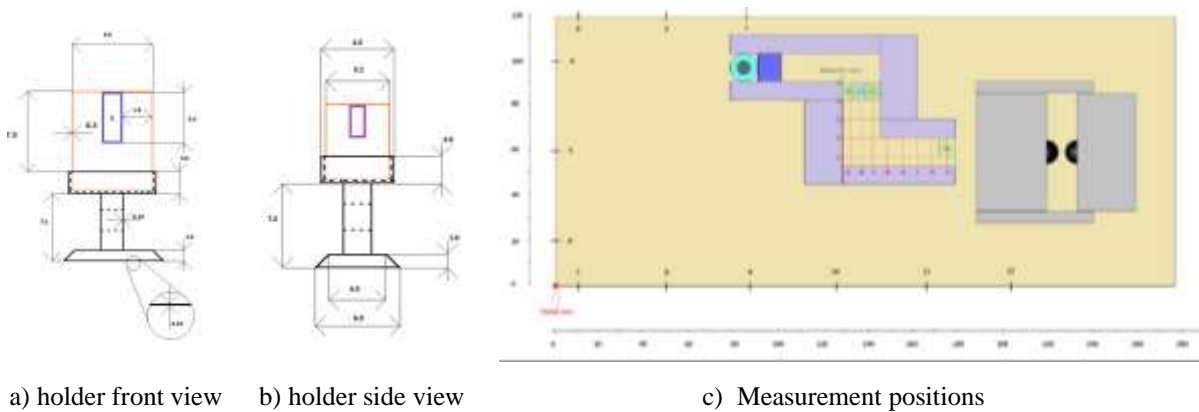


Figure 3: Details of the source holder and PLA tank [5]

The measurement positions inside the Mini Labyrinth are graphically shown in Fig. 3-c). Their tabulated positions (Tab. 1) are relative to the global zero and represent the position of the detector zero. This position is the bottom front left corner of the detector unit. The grey dot in Fig. 3-c) represents the location of the detector zero in the case of the A1 measurement position. The blue and green hatched squares in Fig. 3-c) represent the detector units placed in the model. It should be noted that the real detector holder footprints at A/B and B/C positions overlap, while C/D, D/E, E/F, F/G and G/H are next to each other. Due to overlaps and the influence of multiple detectors, each position should be calculated separately.

Table 1: Measurement positions inside the Labyrinth

Position	X [cm]	Y [cm]	Z [cm]
A1	130.0	93.0	77.5
B1	135.0	93.0	77.5
C1	140.0	93.0	77.5
A2	130.0	85.0	77.5
B2	135.0	85.0	77.5

C2	140.0	85.0	77.5
A3	130.0	77.0	77.5
B3	135.0	77.0	77.5
C3	140.0	77.0	77.5
A4	130.0	69.0	77.5
B4	135.0	69.0	77.5
C4	140.0	69.0	77.5
D4	146.0	69.0	77.5
E4	152.0	69.0	77.5
F4	158.0	69.0	77.5
G4	164.0	69.0	77.5
H4	172.0	69.0	77.5

2.2 Material model - V2

The PuBe source with the neutron emittance of $1.06E7 \text{ n.s}^{-1}$ is used in the experiment. The geometry of the source can be modelled as a void 2 cm high cylinder with 1 cm radius. The related probability density functions (PDF) with energy abscissa values for the neutron and gamma source used by STU team can be found in Tab. 2 and Tab. 3.

Table 2: PuBe neutron emission specification

E [eV]	5.00E+05	1.00E+06	1.50E+06	2.00E+06	2.50E+06	3.00E+06	3.50E+06	4.00E+06	4.50E+06	5.00E+06	5.50E+06
PDF	1.15E-02	3.66E-02	3.21E-02	3.32E-02	4.61E-02	8.88E-02	1.06E-01	9.40E-02	8.47E-02	7.48E-02	4.86E-02
E [eV]	6.00E+06	6.50E+06	7.00E+06	7.50E+06	8.00E+06	8.50E+06	9.00E+06	9.50E+06	1.00E+07	1.05E+07	1.10E+07
PDF	3.84E-02	4.27E-02	5.08E-02	5.06E-02	4.63E-02	3.80E-02	3.34E-02	2.73E-02	1.23E-02	4.00E-03	1.21E-04

Table 3: PuBe gamma emission specification

S [photons/s]	6.89E+06
E [eV]	PDF
3.43E+06	3.21E-01
3.93E+06	4.01E-01
4.44E+06	2.78E-01

To ease the modelling, the material specifications in the form suitable for the SCALE6 [7] computational system are show in Tab. 4.

Table 4: Specification of materials used in the model

atomnylon (SCALE notation)			
·	roth	1.1500	specified density
·	temp	300.0	deg kelvin
	o	6000	12.00 atoms/molecule
	o	7014	2.00 atoms/molecule
	o	8016	2.00 atoms/molecule
wtptneutronstop			
·	roth	1.0568	specified density
·	temp	300.0	deg kelvin
	o	1001	11.597 wt%
	o	5010	0.992 wt%
	o	5011	3.993 wt%

	o	6000	61.283 wt%
	o	8016	22.135 wt%
graphite	·	roth	1.75 specified density
	·	temp	300.0 deg kelvin
	o	6000	1.00 atom/molecule
	•	TSL	
atompla	·	roth	1.4300 specified density
	·	temp	300.0 deg kelvin
	o	6000	6.00 atoms/molecule
	o	1001	8.00 atoms/molecule
	o	8016	4.00 atoms/molecule
plexiglas	·	roth	1.1800 theoretical density
	·	temp	300.0 deg kelvin
	o	1001	8.00 atoms/molecule
	o	6000	5.00 atoms/molecule
	o	8016	2.00 atoms/molecule
dry-air	·	roth	0.0012 theoretical density
	·	temp	300.0 deg kelvin
	o	6000	0.013 wt%
	o	7014	76.508 wt%
	o	8016	23.479 wt%
h2o	·	roth	0.9982 theoretical density
	·	temp	300.0 deg kelvin
	o	1001	2.00 atoms/molecule
	o	8016	1.00 atom/molecule
	o	TSL	
wtpbf3-nat	·	roth	0.0027 specified density
	·	temp	300.0 deg kelvin
	o	5010	2.940 wt%
	o	5011	13.010 wt%
	o	9019	84.050 wt%

2.3 Results - V2

The results of the measurement and computational efforts utilizing the MCNP6 [8] and SCALE6 codes were thoroughly described in [9], thus here just the most relevant results are shown. The neutron flux mesh tallies (the top view at the level of neutron source) calculated in the SCALE 6.2.4 MONACO and CE library are shown in Fig. 4. It can be clearly seen, that the NEUTRONSTOP shielding blocks significantly disrupt the neutron field, which is even more amplified by the presence of the graphite prism at the outside corridor from the labyrinth structure.

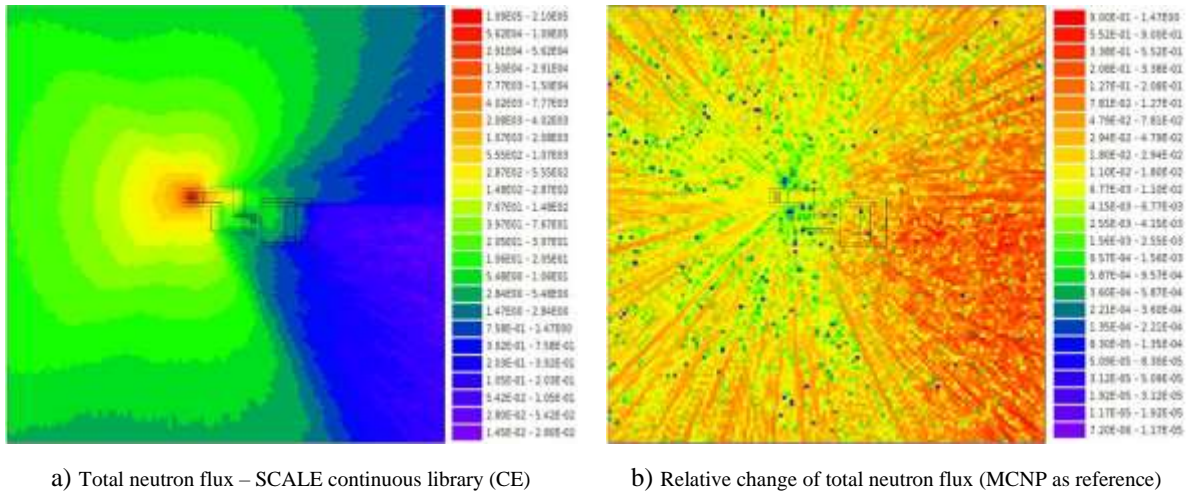


Figure 4: Total neutron flux and relative change between MCNP and SCALE

The relative change $((MCNP-SCALE)/MCNP)$ of the mesh tallies of total neutron flux from MONACO CE and MCNP CE simulations is shown in Fig. 5. It was concluded that the match between both codes inside the labyrinth structure is acceptable and well below 2 %.

The cross-section-induced uncertainties to the calculated ambient dose equivalents from neutrons and photons were also evaluated using SAMPLER supersequence. The one sigma range of cross-section induced uncertainty to the ambient dose equivalent from neutrons was estimated to 1.48 %, while the one sigma range of uncertainty to ambient dose equivalent from photons of 0.59 % was considerably smaller. Interestingly, due to the energy dependence of flux-to-dose factors, the cross-section-induced uncertainties to the integral neutron flux were approx. 1.5 times smaller than in the case of ambient equivalent dose. In the case of photons, the cross cross-section-induced uncertainties were comparable in both cases. In total, 171 independent perturbed calculations were run to estimate the above-mentioned values.

The comparison of the measured and simulated (MCNP CE and SCALE MG) thermal neutron count rates was also carried out. The figures include the results from both calculation codes the RadEye detector and the SNM-11 corona neutron counter. The MT107 (n,α) nuclear reaction rate for thermal neutrons was used as a comparison quantity between simulations and measurement with SNM-11 detector. In case of SNM-11 the measurement of thermal neutrons was carried out in two steps, with the bare detector and with Cd cover.

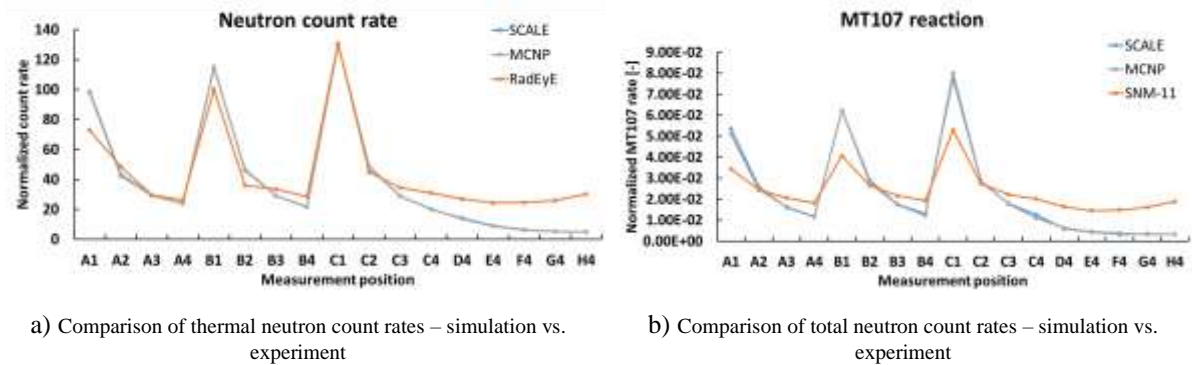


Figure 5: Total neutron flux and relative change between MCNP and SCALE

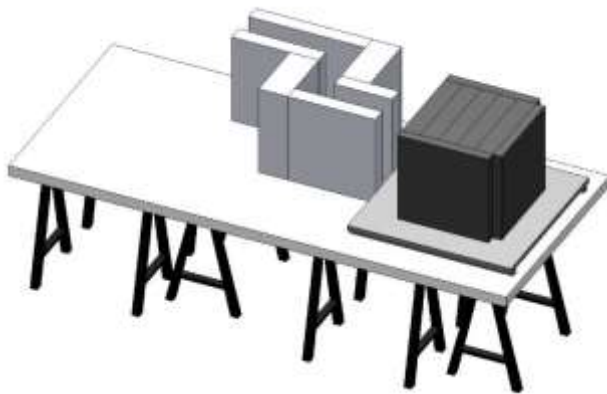
The quantity used for comparison (thermal neutrons rate) was determined by subtracting the results with the Cd cover from the ones obtained for the bare detector. The final graphical

comparison can be found in Fig. 5-a) for RadEyE and Fig. 5-b) for SNM-11. The measurements points are connected for better understanding of trends. Both of the comparisons suggest the need of additional work, where the room effect should be properly taken into account in simulations. The almost perfect match was achieved in the case of comparison of normalized photon count rates. Here just one larger discrepancy at position C1 was identified, other positions show very good performance.

3 THE MINI LABYRINTH V3

3.1 Upgrades

Due to the gained experience and identified influence of the room effect [10] to the experiment, two upgrades were proposed and implemented. First to minimize the backscattering of neutrons from other equipment and concrete walls, the height of the labyrinth walls was doubled to 50 cm. To ease the operation of the graphite blocks, aluminium platform was constructed and installed under the movable part (the SCALE calculation model was also upgraded – see. Fig. 6-a). The distance between the graphite prism and the NEURONSTOP blocks was also modified to 20 cm. To simplify the placement of detectors a new robotic detector positioning mechanism was constructed. Currently, it is possible to move the detector along the specific path in X, Y and Z directions as well as perform the whole measurement in multiple positions fully automatically.



a) Upgraded simulation model

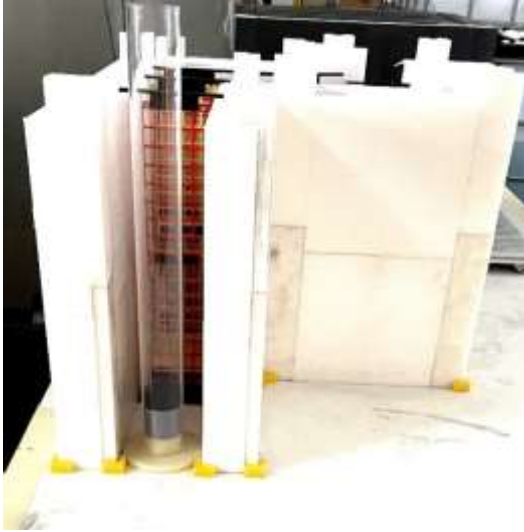


b) Detector positioning system

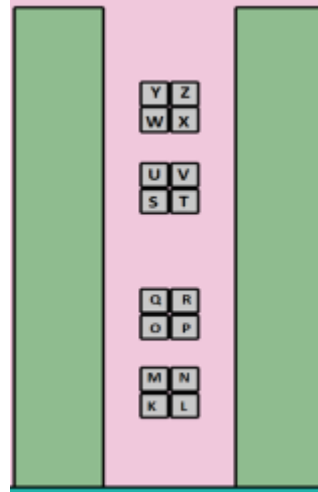
Figure 6: Upgrades implemented to the Mini Labyrinth benchmark

3.2 Measurement utilizing solid-state nuclear track detectors

Thanks to the newly acquired TASLImage™ neutron dosimetry system at INPE, a new neutron measurement option can be utilized for the Mini Labyrinth. Details about the calibration method, etching conditions and other can be found in our previous work [11]. In total, 7 measurement positions are used, all inside the Mini Labyrinth. For these measurements the PuBe source is placed from the left side of the Mini Labyrinth without moderator. The CR-39 detector types were fixed in the 3D printed holder shown in Fig. 7-a) always parallel to the Labyrinth entrance. As shown in Fig. 7-b, 16 CR-39 samples (denoted as K, ...Z) were placed in the holder at 4 different heights (10.1 cm, 18.1 cm, 31. cm and 39.7 cm).



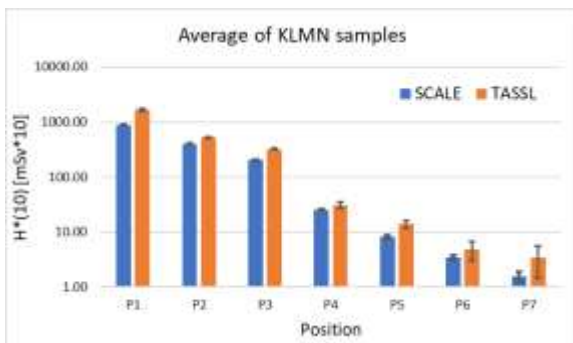
a) 3D printed holder for CR-39 samples



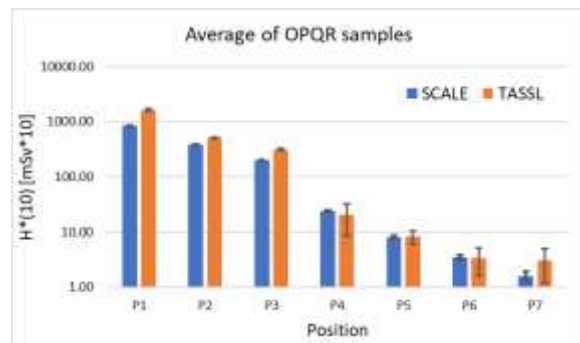
b) Position of the samples from 3D model

Figure 7: Holder and position of CR-39 samples used in the measurement

The measurement positions were situated in the following distances on the x- axis from the entrance of the Mini Labyrinth: 28 cm, 41 cm, 56 cm (in line with entrance corridor), 56 cm (in the middle of y corridor), 56 cm (in line with exit corridor), 75 cm and 90 cm). The samples were irradiated for 23 hours, where the calibration samples were irradiated almost 53 hours with the same neutron source outside the Mini Labyrinth. The calibration value of 5.23 mSv $H^*(10)$ was determined by the NUDET-ENE [12] detector placed in the same distance from the neutron source. The simulation of the response $H^*(10)$ was performed by SCALE6 system as in the previous case, where all CR-39 samples were modelled as point detectors. For the sake of brevity, the acquired doses of the group of 4 samples (e.g., KLMN) were averaged for graphical processing. The results of the 4 heights and all positions in the labyrinth (P1, .. P7) are shown in following Fig. 8-9. To ease the readability, the y-axis values are multiplied by the factor of 10.



a) KLMN



b) OPQR

Figure 8: Comparison of doses determined by TASSL and SCALE – part 1

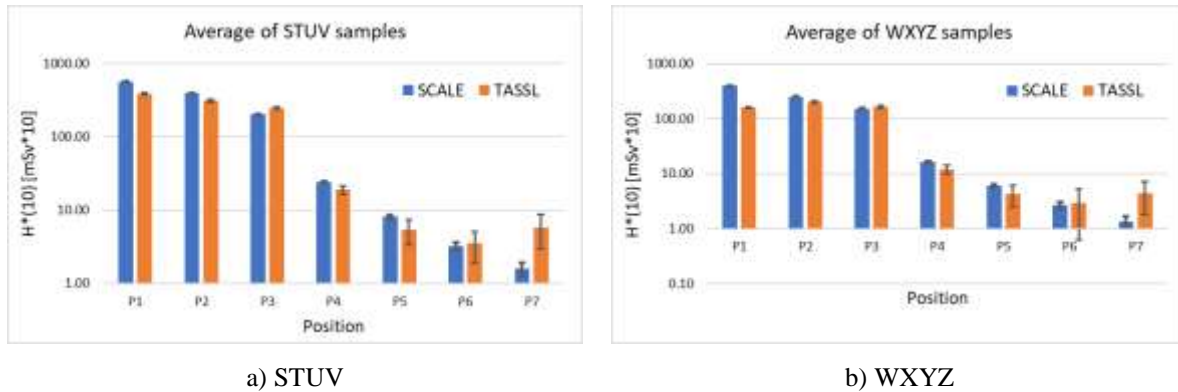


Figure 9: Comparison of doses determined by TASSL and SCALE – part 2

We can conclude that the results gained showed the same trends for almost all positions. The relevant difference can be found mainly in the P7 position which is located at the very end of exit corridor. Here the doses measured are near the detection limit of CR-39 detectors. Moreover, the large water tank is placed nearby in the laboratory, thus room effect might play the role. The relative change between the doses measured and calculated is about 30 % except for the position P1, where the results differ almost by 50 %. The axial distribution of the dose in the corridor significantly differs between the simulation and experiment. This might be caused by the neglect of the neutron source anisotropy in the simulation or by the relevant room effect (laboratory floor is much closer than ceiling). These aspects need to be investigated further.

4 CONCLUSIONS

In order to enhance the capabilities of STU in radiation shielding, to provide more opportunities for the next generation of students to experience radiation protection principles in practice as well as to validate computer codes, the Mini Labyrinth experiment is developed under the international framework. It was inspired by the ALARM-CF-AIR-LAB-001 ICSBEP experiment, is made from NEUTRONSTOP shielding blocks and can be used for measurements using active and passive neutron detectors with thermal and fast neutrons. The development is performed step by step. The first version was aimed on demonstrating the basic principles (V1). Subsequently, the second (V2) version reached the level of a simple benchmark experiment. The measurements and simulations performed on this version identified important areas for improvement. The last version (V3) presented in this paper, incorporates the previous findings and is now ready to demonstrate radiation shielding in practice and will be used as part of the online education process under the Erasmus+ project PADINE-TT. In this paper, we presented the geometry specification of the experiment and results of experimental measurements and simulations using the SCALE6 MONACO and MCNP6 codes. In terms of simulations, it was found, that both codes can be used for simulations of the Mini Labyrinth with acceptable precision and can also serve for the verification of experimental results. The precision of the codes was evaluated through the calculation of neutron and gamma fluxes, ambient dose equivalent rates and reaction rates of interest. Using SCALE6, also cross-section-induced uncertainties were estimated. Recently also measurements with CR-39 solid-state track detectors were performed that confirmed the applicability of this method. After gaining further experience, this method will provide new opportunities for the development of the STU workplace.

ACKNOWLEDGMENTS

This study has partially been financially supported by the Slovak Research Development Agency by projects No. APVV 20-0300, No. APVV DS-FR-19-0014, No. APVV 21-0170 and by the Scientific Grant Agency of the Ministry of Education of Slovak Republic No. VEGA 1/0615/21.

REFERENCES

- [1] I. A. Kodeli et al., "SINBAD – Radiation shielding benchmark experiments", *Annals of Nuclear Energy*, 159, 2021.
- [2] OECD NEA, *International Handbook of Evaluated Critical Safety Benchmark Experiments*, OECD, Paris, 2020.
- [3] KOPOS a.s., *Shielding bricks NEUTRONSTOP*, 2022, [Online]. Available: https://www.kopos.sk/sites/default/files/catalog/2017/10/neu_en_stinici_tvarovsky_neutr_ostop.pdf. Accessed on: September 8, 2022.
- [4] Š. Čerba et al., "Preliminary Results of the STU Mini Labyrinth Radiation Shielding Experiment", *AIP Conference Proceedings*, 2411, 2021.
- [5] Š. Čerba et al., *Mini Labyrinth V02 – PuBe*, STU, Bratislava, 2021 (non-public).
- [6] Thermo Scientific, *RadEye SPRD Personal Radiation Detector*, 2021, [Online]. Available: <https://www.thermofisher.com/order/catalog/product/4250817#/4250817>. September 8, 2022.
- [7] W. A. Wieselquist, et al., *SCALE Code System*, ORNL/TM-2005/39, Version 6.2.4, Oak Ridge National Laboratory, Oak Ridge, TN, 2020.
- [8] C. H. Warner, et al., *MCNP 6.2 Release Notes*, LA-UR-18-20808, Los Alamos National Laboratory, Los Alamos, 2018.
- [9] B. Vrban et al., "The Mini Labyrinth Benchmark for Radiation Protection and Shielding Analysis", *IEEE Transactions on Nuclear Science*, 69, 2022, pp. 745-752.
- [10] Š. Čerba et al., "Measurement and Simulation of the Mini Labyrinth experimental workplace at STU", *Radiation Protection Dosimetry*, 198, 2022, pp. 628-633.
- [11] B. Vrban et al., "Response of Plastic Track Detector of the TASTRAK Type to Neutrons of Pu-Be source", *Radiation Protection Dosimetry*, 198, 2022, pp. 687-692.
- [12] Nuviotech Instruments, *Nudet Neutron*, 2022, [Online]. Available: <https://www.nuviotech-instruments.com/product/nudet-neutron/>. Accessed on: September 8, 2022.